Eur Biophys J (2010) 39:299–306
DOI 10.1007/s00249-009-0544-8

ORIGINAL PAPER

Hydrophobicity as a possible reason for gelation of FG-rich nucleoporins

Philipp M. Diesinger · Dieter W. Heermann

Received: 16 March 2009 / Revised: 22 July 2009 / Accepted: 7 September 2009 / Published online: 1 October 2009

Abstract In this work we address the question of whether hydrophobic parts of FG-rich nucleoporins can be the reason for their ability to form a hydro-gel (Frey et al. in Science 314:3, 2006). We focus on the N-terminal fsFG domain of the essential yeast nucleoporin Nsp1p (Hurt in EMBO J 7:4323, 1988) as a nucleoporin model system and on the question of whether a phase transition between a sol and a gel phase exists. The N-terminal fsFG domain comprises 18 regular FSFG repeats and 16 less regular FG repeats. This domain is modeled, and a Metropolis Monte-Carlo algorithm is used to generate equilibrated ensembles of peptide networks, which were then analyzed by percolation theoretical methods. We take into account the excluded volume of the protein backbone and all side chains that are at least medium-sized (starting with Glu/E) as well as the hydrophobic clusters of the amino acid sequence. There is a competition between two kinds of entropic forces in the system: the excluded volume interactions and the hydrophobic parts of the nucleoporin strands. Therefore, it is not a priori clear whether the system percolates at a biologically realistic density. Nevertheless, we find a sol–gel phase transition in the system at a critical density of 42 mg mL^{-1}. This may be considered a hint that hydrophobic nucleoporin parts are key for the formation of gels in the nuclear pore complex.

Keywords Monte Carlo · Nsp1p · Nucleoporin · Percolation · Nsp1p

P. M. Diesinger (✉) · D. W. Heermann
Department of Physics,
Institut für Theoretische Physik,
Universität Heidelberg, Philosophenweg 19,
69120 Heidelberg, Germany
e-mail: diesinger@tphys.uni-heidelberg.de;
p.m.diesinger@gmx.de

D. W. Heermann
Interdisziplinäres Zentrum für Wissenschaftliches Rechnen,
Universität Heidelberg,
Heidelberg, Germany

Introduction

All the proteins of the cell nucleus are imported from the cytoplasm. At the same time, the nucleus supplies the cytoplasm with all kinds of nuclear products such as messenger RNA or transfer RNA. Since, during interphase, the eucaryotic cell nucleus is surrounded by a double membrane called the nuclear envelope (NE), transport between the cytoplasm and the nucleus has to proceed through specialized pores. Such pores are built by so-called nuclear pore complexes (NPCs), large proteinaceous channels distributed across the NE. About 2,000 such NPCs exist on average within the nuclear envelope of a vertebrate cell. Their exact number varies depending on cell type and throughout the cellular life cycle.

The central aqueous channel within NPCs is 40–60 nm in length and has a diameter of 30–50 nm depending on the organism. This channel is guarded by a permeability barrier (Görlich and Kutay 1999; Macara 2001) that prevents uncontrolled intermixing of cytoplasmic and

nuclear contents by effectively blocking diffusion of particles larger than 30–40 kD in size. At the same time, however, this barrier allows efficient passage of molecules that are in complex with nuclear transport receptors (NTRs) (Görlich and Kutay 1999; Pemberton and Paschal 2005; Weis 2002). This facilitated mode of NPC passage is reliant on interactions of NTRs with the FG-rich nucleoporin repeats (Radu et al. 1995; Iovine et al. 1995; Bayliss et al. 1999; Bayliss et al. 2000; Bednenko et al. 2003).

Each NPC is built up from multiple copies of a set of about 30 different proteins collectively called nucleoporins. About half of these nucleoporins predominantly consist of folded domains often displaying alpha solenoid- or beta-propeller folds. The second half also contains domains that show structural characteristics typical of intrinsically unfolded proteins (Denning et al. 2003), i.e., highly flexible elements lacking ordered secondary structure (Denning et al. 2003). Such unstructured domains typically consist of up to 50 phenylalanine-glycine (FG) dipeptide motifs (Peters 2006; Rout and Wente 1994) spaced by hydrophilic amino acid stretches and are therefore called FG-rich nucleoporin repeat domains.

Although it is commonly accepted that the permeability barrier consists of FG-rich nucleoporin repeat domains, several different models exist that try to explain how such repeats can form an efficient barrier.

These models (Macara 2001; Rout et al. 2000; Ribbeck and Görlich 2001, 2002) differ foremost in the question of whether the permeability barrier is tightened by inter-repeat interactions or not. The "selective-phase" model (Ribbeck and Görlich 2001, 2002) assumes the barrier to be a sievelike structure, formed by hydrophobic interactions between the hydrophobic clusters of the FG repeats. Then the sieve's mesh size predetermines a size limit for passive exclusion. NTRs could bypass this size restriction since their binding to hydrophobic clusters competes with the noncovalent inter-repeat cross-links and, thereby, opens adjacent meshes of the sieve.

All other models have in common that they neglect interactions between FG-repeat domains. Recent attempts to discriminate between the proposed models experimentally were based on the simple assumption that without inter-repeat interactions, aqueous solutions of FG-repeat domains should behave like viscous fluids. In contrast, if cross-linking prevented a free sliding between the linear polymers, an elastic hydrogel should form. Frey et al. (2006) tested these predictions for the N-terminal fsFG-repeat domain of the essential yeast nucleoporin Nsp1p, which comprises 18 regular FSFG repeats and less regular FG repeats (Hurt 1988):

MNFNTPQQ
NKTPFSFGTANNNSNTTNQNSST
GAGAFGT
GQSTFGFNNSAPNNTNNANSS
ITPAFGSNNT
GNTAFGNSNP
TSNVFGSNNS
TTNTFGSNSA
GTSLFGSSSAQQTKSNGTA
GGNTFGSSSLFNNSTNSNT
TKPAFGGLNFGGGNNTTPSSTGNANT
SNNLFGATANANK
PAFSFGATTNDDKKTEPDK
PAFSFNSSVGNKTDAQAPT
TGFSFGSQLGGNKTVNEAAK
PSLSFGSGSAGANPAGASQPEPTTNEPAK
PALSFGTATSDNKTTNTT
PSFSFGAKSDENKAGATSK
PAFSFGAKPEEKKDDNSSK
PAFSFGAKSNEDKQDGTAK
PAFSFGAKPAEKNNNETSK
PAFSFGAKSDEKKDGDASK
PAFSFGAKPDENKASATSK
PAFSFGAKPEEKKDDNSSK
PAFSFGAKSNEDKQDGTAK
PAFSFGAKPAEKNNNETSK
PAFSFGAKSDEKKDGDASK
PAFSFGAKSDEKKDSDSSK
PAFSFGTKSNEKKDSGSSK
PAFSFGAKPDEKKNDEVSK
PAFSFGAKANEKKESDESK
SAFSFGSKPTGKEEGDGAK
AAISFGAKPEEQKSSDTSK
PAFTFGAQKDNEKKTEESSTG

(Hydrophobic clusters we considered are marked blue whereas the amino acids the side chains of which were allowed for are marked red.)

They showed that a macroscopic gel is indeed formed when the protein concentration exceeds 8–10 mg mL^{-1} of repeat domains (Frey, pers. comm.).

The same repeat domain will be considered here as an FG-rich model system. We want to address the question as to whether the interactions of the hydrophobic FG-rich repeats are actually strong enough to form a hydrogel. These attractive cluster-forming interactions are in strong competition with the repelling (entropic) forces caused by excluded volume of the nucleoporins and their side chains so that it is not a priori clear whether the system shows a transition from the sol to the gel state (Flory 1947) at a biologically realistic density. In contrast to the colloid sol state, gel formation would argue for a substantially dilute cross-linked system.

Answering this question will give important information about possible implications of hydrophobic interactions for the gelation of nucleoporin FG-repeat domains. Furthermore, one can examine whether the system is in the 3D percolation universality class. Finally, a finite size scaling will supply the order of magnitude of the critical density at which the phase transition lies since we are interested in modeling the main effect here and do not want to go too much into details to keep the simulations fast.

Theory

Sol–gel transition as a percolation problem

FG-rich parts of nucleoporins in water have the ability to cluster together due to their strong hydrophobicity

(Ben-Naím 1980). Therefore, two or more different peptide chains can coalesce via hydrophobic bonds to form a cluster (cf. Figs. 1, 2). On the other hand, repellent forces, such as from the excluded volume of the peptide backbone or the side chains, counteract this effect. The mixture of peptide chains with the water molecules and possibly already existing small peptide clusters represents the sol phase. In sol systems (Sahimi 1994; Stauffer and Amnon 1992), it happens that as the mass density c of the monomers (or even polymers) increases, larger and larger clusters are formed.

We want to examine whether the hydrophobic clustering can become so strong that it leads to a phase transition of the system. If this is the case, the system develops macroscopic properties such as a finite elasticity or shear modulus (Stauffer and Amnon 1992; Sahimi 1994) when the density exceeds a critical value c_{crit}. At the phase transition, a large cluster will exist that represents the gel network and often coexists with single unbound peptide chains that may even be trapped in the interior of the gel (cf. Fig. 2). Further increasing of the density will let the sol phase disappear completely and eventually all peptides will contribute to one large cluster, i.e., the gel network.

In the case of such a sol–gel phase transition, the critical density signals a connectivity transition of the system. This model of polymerization and gelation was first invented by Flory (1941, 1947) and Stockmayer (1943) who were interested in the formation of large branched polymers.

Physical gels, in contrast to chemical gels, are formed when no permanent chemical reaction takes place between the monomers (or polymers). Instead only a reversible association links the particles to each other. Examples are silica aerogels and structures formed during the gelation of silica particles in pure water or NaCl solution (Sahimi 1994). We will also allow hydrophobic bonds between peptides to be dissolved again by thermic fluctuations (see below). In all these examples, the connectivity properties of the system play a key role in understanding them physically.

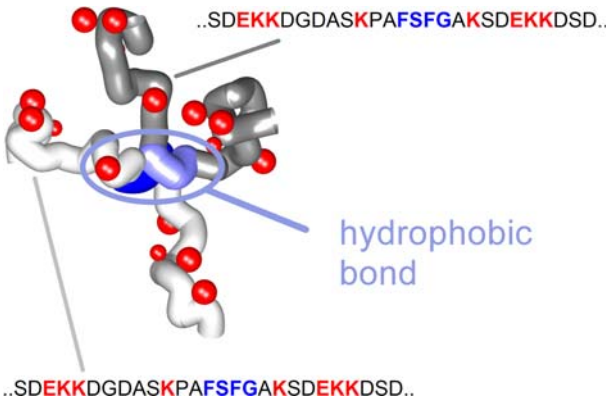

Fig. 1 Two parts (colored *white* and *gray*) of the N-terminal fsFG domain of the essential yeast nucleoporin Nsp1p coalesce around a hydrophobic bond and thus form a cluster. The *blue* parts of the peptide backbone mark hydrophobic regions. The *red* spheres illustrate the positions of the side chains (that are at least medium sized). The corresponding amino acid sequences of the illustrated nucleoporin parts are shown too and have the same *color code* as in the cluster visualization

Percolation theoretical methods to examine connectivity properties

If a transition from a sol phase with only a few clusters to a gel phase with cross-linked peptides exists, increasing the mass density c of the system over some critical density c_{crit} would push the system from the colloidal sol state to a gel state (Stauffer and Amnon 1992). To determine whether the system has such a phase transition from a sol to a gel state we develop a model and then apply percolation theoretical methods (Stauffer and Amnon 1992; Flory 1947) to analyze the data.

Here we have to examine the hydrophobic cross-linking between peptide chains. Two important properties in this context are the correlation length $\xi(c)$ and the percolation probability $P_\infty(c)$ of the system. In cases where the linear dimension of the system l is larger than the correlation length, ξ is a measure of the largest hole in the largest cluster, and it decreases as c is increased above c_{crit}. P_∞ is the probability that a given peptide belongs to the largest cluster of the system.

Near the percolation threshold of infinitely large systems, i.e., as c approaches c_{crit}, most percolation quantities obey scaling laws that are largely insensitive to the structure and the microscopic details of the system. For example the correlation length and P_∞ scale as

$$\xi \propto |c - c_{crit}|^{-\nu} \quad \text{and} \quad P_\infty \propto (c - c_{crit})^{\beta}.$$

Here ν and β are critical exponents that are completely universal, i.e., they are independent of the microscopic details of the system and depend only on the dimensionality. Even long but finite range interactions do not change this universality although they may change the value of c_{crit}. The prefactors are nonuniversal (although certain ratios of them are universal again) and therefore not mentioned here. Although percolation is universal, c_{crit} is very difficult to measure and depends on the microscopic details of the system. Our main question in this work is whether such a critical density and thus a phase transition exists at all.

For an infinite system, P_∞ behaves as $P_\infty \propto (c - c_{\text{crit}})^{\beta}$ if the density approaches the critical value. As the mass density is decreased to the critical value, P_∞ decreases to zero. For $c < c_{\text{crit}}$, P_∞ is zero. In a finite system, as c_{crit} is approached, ξ eventually becomes comparable to the linear

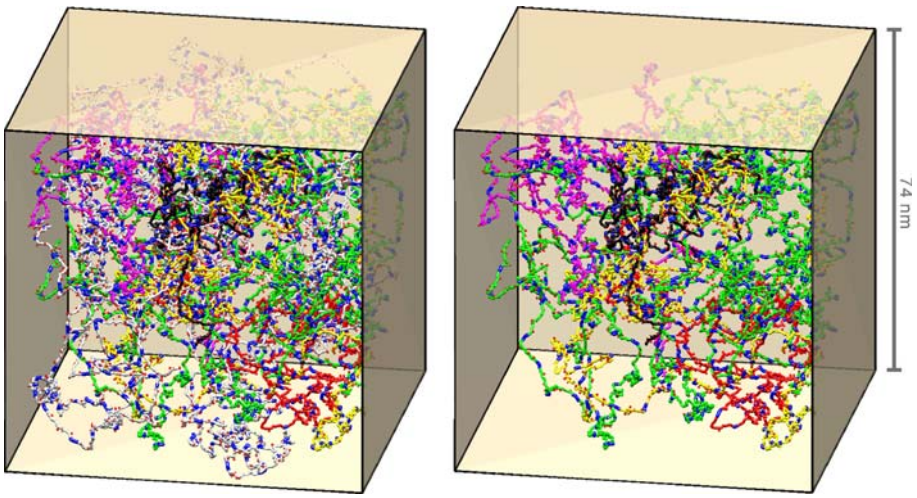

Fig. 2 Example configuration of 40 peptides (N-terminal Nsp1p fsFG domains) with colored clusters at a mass density of 10 mg mL^{-1}. Altogether there are five clusters [colored *green* (12 peptides), *yellow* (5 peptides), *red* (2 peptides), *black* (2 peptides), and *pink* (3 peptides)] in this configuration. *White* peptides are single, unbound nucleoporins that have no hydrophobic bond with another peptide and thus do not contribute to any cluster. The box on the *right* shows the same configuration as on the *left* with the difference that the single unbound peptide chains are not shown. Sixty percent of all nucleoporins in this configuration have hydrophobic bonds, i.e. they contribute to some of the five clusters. The other 40% are unbound

size of the network. Therefore, the variation of any property X of a system of linear size L is given by

$$X \propto L^{-a} f(x),$$

where $x = L^{1/\nu}(c - c_{\text{crit}})$ and $f(0)$ is nonsingular (Fisher 1971; Stauffer and Amnon 1992). One can use this equation either to determine critical exponents or to estimate the critical density itself. The latter is done here.

Near c_{crit} and over the limit $L \to \infty$, $P_\infty \propto (c - c_{\text{crit}})^\beta$ (Stauffer and Amnon 1992). This leads to $a = \frac{\beta}{\nu}$. Therefore, all different system sizes we simulated fulfill the condition

$$P_\infty L^{\beta/\nu} \propto f(L^{1/\nu}(c - c_{crit})). \quad (1)$$

This means variation of c_{crit} until all curves f for the different system sizes collapse to a master curve supplies the critical mass density at which the percolation threshold lies.

Methods

In the model we take into account all FG-rich hydrophobic clusters of the nucleoporin strands. An individual Nsp1p peptide chain is shown in Fig. 3. Every single chain consists of 606 amino acids, has a mass of 62,116.1 Da and consists of 37 hydrophobic clusters, i.e., 110 hydrophobic amino acids. The hydrophobicity is modeled similarly to the hydrophobic-polar protein folding model (Dill 1985). If two hydrophobic parts of the peptide chains come closer than 0.7 nm, the total energy of the system is reduced by 0.04336 eV (Ben-Naím 1980; Kyte and Doolittle 1982). Furthermore, the excluded volume of every amino acid is factored in just like the side chains of all large and medium amino acids (starting at Glu/E). All smaller side chains were neglected. The peptide backbone is modeled as a tube with side chains and hard-core excluded volume potential, i.e., two peptide chains are not able to penetrate each other. The amino side chains are modeled as spheres attached to the tube-like peptide backbone. The radius of the sphere depends on the size of the corresponding side chain. Furthermore, all chains are trapped in a cube with side length l (cf. Figs. 2, 4). The formation of hydrogen bonds as well as hydrophobic or hydrophilic interactions other than those of the FG repeats is neglected in this model. Our model is not limited to an underlying spatial lattice.

The rotational freedom (Φ and Ψ) of the peptide bonds between sp^3 and sp^2 hybridization of each amino acid is modeled by pivoting the nucleoporin strand with respect to the excluded volume potentials. Every amino acid contributes to the peptide flexibility with one joint of this kind.

We used a Metropolis-Hastings Monte-Carlo algorithm to generate many equilibrated configurations of our nucleoporin model system (the N-terminal fsFG domain of the essential yeast nucleoporin Nsp1p) at various densities to analyze their connectivity properties.

The Metropolis algorithm is a rejection sampling algorithm used to generate a sequence of samples from a probability distribution that is difficult to sample from directly. We used it to generate equilibrated ensembles of

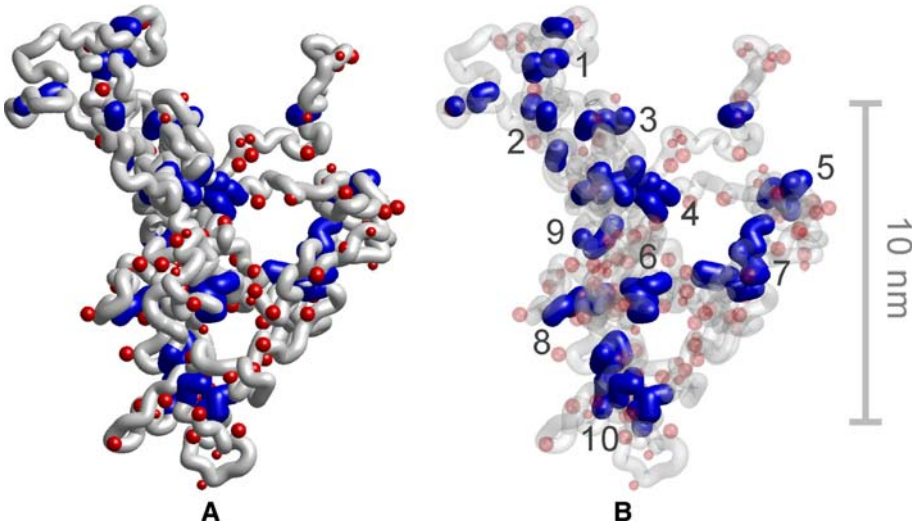

Fig. 3 **a** One conformation (out of the whole ensemble) of a single nucleoporin strand. The *red* spheres represent side chains of large and medium amino acids (starting with Glu/E). The FG-rich hydrophobic parts of the nucleoporin are marked *blue*. They have been enlarged by 30% for this visualization. **b** Same as **a** but with transparent backbone and amino acid side chains to give a better view of the hydrophobic parts. One can see small hydrophobic clusters (numbered *1–10*). Since there is no other peptide chain, these are intra-bonds (cf. Fig. 7), i.e., bonds that the peptide coalesces with itself

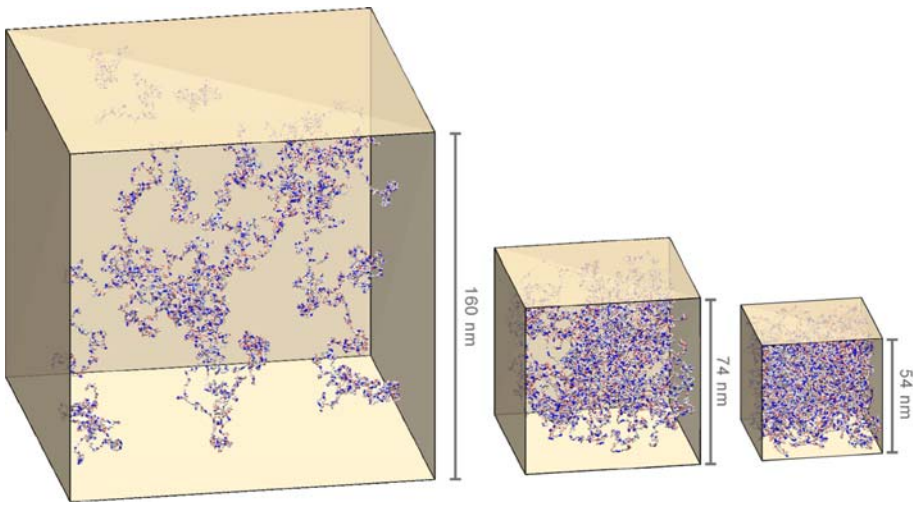

Fig. 4 Three example configurations of a system with 40 peptides with different box sizes and thus different mass densities (1, 10, and 25 mg mL^{-1}). The clustering of the peptide chains increases (the fractions of clustered peptides are 10, 37.5, and 72.5% with decreasing density (and decreasing box volume)

peptide networks of a given density and temperature with Maxwell–Boltzmann distributed energy. The start configuration for every peptide chain is a self-avoiding random walk. The algorithm uses pivot moves to alter the peptide chains during the iterations as described above. Randomly a number of peptide chains is chosen and pivoted (with respect to the excluded volume interactions). Then the energy difference ΔE between the new state after and the old state before the pivot moves is calculated. At the end of the step, a random variable decides with respect to the Maxwell–Boltzmann distribution whether the new state is accepted or rejected. Hereby, the acceptance probability is

$$p_A = \min\left(1, \exp\left(-\frac{\Delta E}{kT}\right)\right),$$

where k is the Boltzmann constant. This last step allows thermal fluctuations to break bonds and dissolve clusters with a certain probability. Thus, one gets equilibrated ensembles of system configurations at a certain density c and a temperature T. The latter was fixed at $T = 300$ K (i.e., lab conditions).

Then one can average over such an ensemble to determine system properties such as P_∞ or the radius of gyration, which is a measure of the extension of the system. The radius of gyration is defined by

$$R_g^2 = \frac{1}{M}\int d^3 r \rho(\vec{r})|\vec{r} - \vec{r}_S|^2,$$

where ρ is the mass density, M the mass, and $\vec{r}_S$ the center of mass. The radius of gyration will be used later in this work.

For every simulated system size ($n = 10, 25, 40, 50$, and 60 peptides), we generated an ensemble of at least 10^5 configurations. Some example configurations are shown in Figs. 3 and 4. The red spheres represent amino acid side chains, whereas the blue tubes show hydrophobic regions. The box surrounding the peptide system has free boundary conditions and its size l is determined by the density c. Figure 3 shows only a single simulated N-terminal Nsp1p fsFG domain. One can see that some hydrophobic clusters are formed, whereas other hydrophobic parts remain unbound. Three different example configurations of peptide systems with 40 peptides are shown in Fig. 4. The configurations have different peptide mass densities. At a low density (on the left), only a few peptides coalesce bonds. But increasing the density leads to an increase in these bonds and thus an increase in peptide clusters in the system. The box on the right of Fig. 3 shows a configuration where all peptides contribute to one large cluster. Hydrophobic bonds can again be dissolved by thermal fluctuations of the system.

Results

Figure 5 shows the increase of clustering in the system. With increasing mass density, the peptide network exceeds the percolation threshold and eventually all chains contribute to one large cluster. Finite size effects lead to a rounding of the phase transition (Stauffer and Amnon 1992). This shows that the attractive cluster-forming hydrophobic interactions of the N-terminal Nsp1 fsFG domains are strong enough to compete with the entropic forces of the excluded volume of the peptide strands. This may be a hint that indeed FG-rich hydrophobic parts of nucleoporins are key for the percolation and thus the formation of gels in the nuclear pore complex.

Figure 6 shows the radius of gyration R_g of the largest cluster. For small densities, R_g is simply the extension of a single peptide chain (about 10 nm) because the chains interact very weakly with each other and therefore collapse by forming hydrophobic clusters. With increasing density, the average largest cluster grows and thus the correlation length increases until one large cluster is formed. Eventually at high densities (i.e., near c_{crit}), the box volume limits extension of the cluster and therefore R_g decreases again as the box size l decreases with increasing density c (as $c \propto l^{-1/3}$).

The average number of hydrophobic bonds that an individual peptide chain coalesces with itself ("intra-bonds") to form hydrophobic clusters is relatively independent of the mass density (cf. Fig. 7). The average number of intra-bonds of a single Nsp1p peptide chain is on the order of 100. However, the average number of hydrophobic bonds that an arbitrary peptide chain coalesces with other peptide chains ("inter-bonds") rapidly increases with the mass density of the system and the system size (cf. Fig. 7).

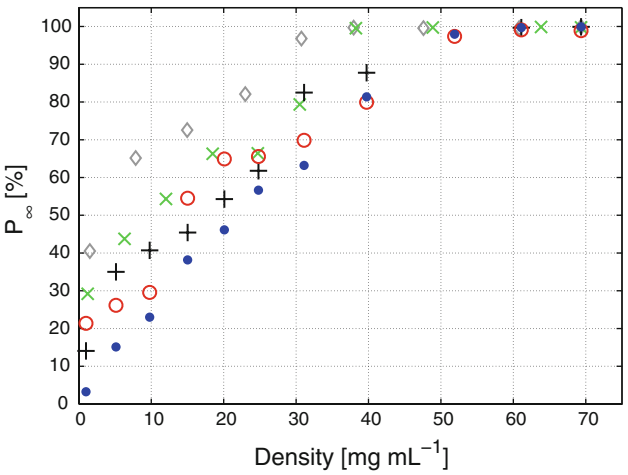

Fig. 5 The average percentage of the largest cluster is dependent on the mass density of the system. One can see that the largest cluster grows with increasing density until all peptides are linked. In this case the system acquires macroscopic properties such as a finite elasticity or shear modulus and thus a gel is formed. *Dots* $n = 10$, *circles* $n = 25$, *plus signs* $n = 40$, $\times$ $n = 50$, *diamonds* $n = 60$

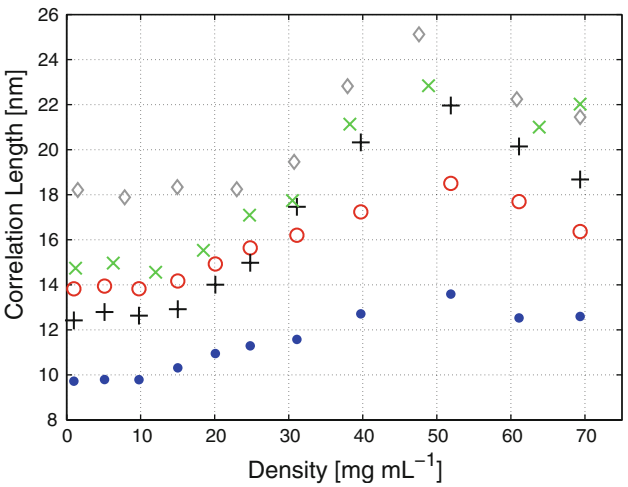

Fig. 6 The mean radius of gyration R_g of the largest cluster of the nucleoporin system as a measure of the system's correlation length in dependence on the mass density. For very small densities the correlation length is just the average extension of a single peptide (around 10 nm). With increasing density, the largest cluster grows and thus the correlation length increases. In the case of large densities ($c > c_{crit}$), the cluster size is eventually limited by the box size l and thus R_g is approximately the linear dimension of the bounding box, which decreases with increasing density c ($c \propto l^{-1/3}$). *Dots* $n = 10$, *circles* $n = 25$, *plus signs* $n = 40$, $\times$ $n = 50$, *diamonds* $n = 60$

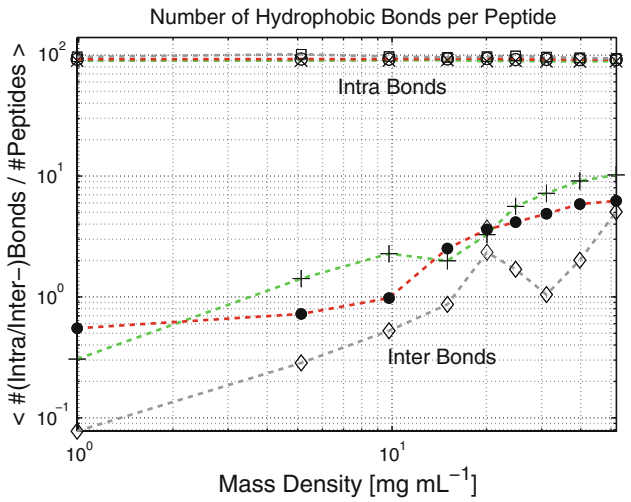

Fig. 7 The average number of bonds between different peptides (*inter*) and the average number of bonds an individual peptide coalesces with itself (*intra*) as a function of the number of peptides in the system. One can clearly see that the number of inter-bonds increases with the mass density whereas the number of intra-bonds is density independent. *Squares* $n = 10$ (intra), *circles* $n = 25$ (intra), $\times$ $n = 40$ (intra), *diamonds* $n = 10$ (inter), *dots* $n = 25$ (inter), *plus signs* $n = 40$ (inter)

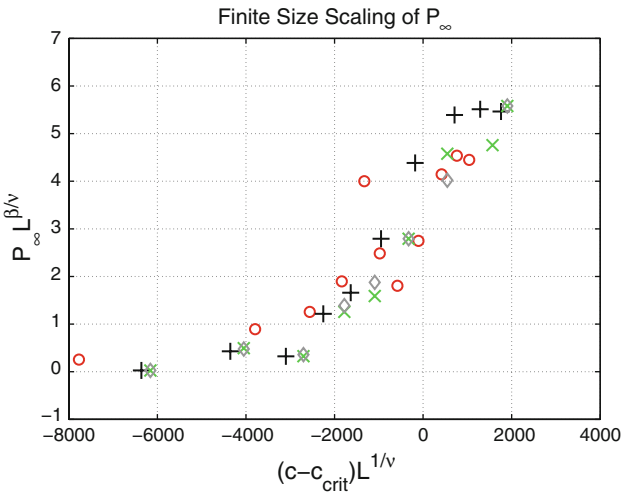

Fig. 8 The finite size scaling of P_∞ which was used to determine the critical density c_{crit}. The latter was considered as a parameter here and varied in integer steps of 1 mg mL^{-1} until the curves for different system sizes fit best upon one another (cf. Eq. 1). The critical density found in this way is $c_{crit} = 42$ mg mL^{-1}. Our focus was on the FG-rich hydrophobic clusters and thus the hydrogen bonds; other hydrophobic or hydrophilic interactions were neglected leaving a margin for this value, but in principle, the order of magnitude should be correct and we proved that gelation is possible. The critical exponents used here were $\beta = 0.41$ and $\nu = 0.88$. *Circles* $n = 25$, *plus signs* $n = 40$, $\times$ $n = 50$, *diamonds* $n = 60$

The finite size scaling of P_∞ is shown in Fig. 8. c_{crit} was varied across integer intervals until the data collapse to the master curve was best. We used the sum of the squared distances between the curves for different system sizes as a measure of the extent of the data collapse and varied c_{crit} until it was minimal. The result for the critical density was $c_{crit} = 42$ mg mL^{-1}. The critical exponents used were $\beta = 0.41$ and $\nu = 0.88$, i.e., the critical exponents of 3D percolation. Other critical exponents give a bad fit. One can see in Fig. 8 that the collapse to a master curve is not perfect but one has to keep in mind that P_∞ has strong fluctuations (cf. Fig. 5). The peptide systems were difficult to sample, and we decided to simulate different system sizes instead of absolutely minimizing fluctuations of the measured properties for only one fixed number of peptides. At the end, this is what makes the finite size scaling possible. The estimation of the critical density is a byproduct of this work. Our main goal was to answer whether there is a phase transition to a gel phase at all.

Discussion

It was not a priori clear whether the examined peptide system would be able to form a gel by hydrophobic FG-rich clusters at biologically realistic densities. In our model system of the Nsp1p fsFG domain, we found a gel–sol phase transition at a critical density of 42 mg mL^{-1}, which is not far from biologically realistic densities in nuclear pore systems. Experiments on Nsp1p systems show that a macroscopic gel is formed above densities of 8–10 mg mL^{-1}. The gel was identified in this case by visual inspection (Frey et al. 2006).

This shows that the attractive cluster-forming hydrophobic interactions of the N-terminal Nsp1 fsFG domains are strong enough to compete with the entropic forces from the excluded volume of the peptide strands. This may be a hint that indeed FG-rich hydrophobic parts of nucleoporins are key for the percolation and thus for the formation of gels in the nuclear pore complex.

We neglected hydrogen bonds in our model as well as hydrophilic interactions and focused instead on modeling the most dominant effects, namely the FG-rich hydrophobic clusters. Hydrogen bonds would support attractive forces whereas hydrophilic parts would lead to an increase in the repulsion in the system and thus to more open structures. These opposite effects might slightly shift the critical density of the system. Exact predictions of critical densities in such complex systems are very difficult even in the easier case of Ising models.

The small number of inter-bonds (compared to the number of intra-bonds) may give the peptide network the possibility of opening up easily, which might be a biological advantage to facilitate transport through the nuclear pore complex.

Although we already invested a huge amount of computer time ($\approx 2 \times 10^4$ h on average CPUs), more

simulations especially of larger systems would be desirable. One could reduce the finite size effects and have a more detailed view of the system. But we would need an order of magnitude more computation time in order to achieve this goal which is not possible with current machines. Nevertheless, the data presented are already sufficient to show that the Nsp1p peptide network is a percolating system and that the percolation threshold lies at the order of magnitude of 40 mg mL^{-1}, which is close to experimental results (Frey et al. 2006).

Acknowledgments We thank the Max-Planck-Institut für Biophysikalische Chemie in Göttingen for funding as well as the Heidelberg Graduate School of Mathematical and Computational Methods for the Sciences for partial funding of Philipp M. Diesinger's work.

References

Bayliss R, Ribbeck K, Akin D, Kent HM, Feldherr CM, Görlich D, Stewart M (1999) Interaction between NTF2 and xFxFG-containing nucleoporins is required to mediate nuclear import of RanGDP. J Mol Biol 293:579–93

Bayliss R, Littlewood T, Stewart M (2000) Structural basis for the interaction between FxFG nucleoporin repeats and importin—in nuclear trafficking. Cell 102:99–108

Bednenko J, Cingolani G, Gerace L (2003) Importin beta contains a COOH-terminal nucleoporin binding region important for nuclear transport. J Cell Biol 162:391–401

Ben-Naím A (1980) Hydrophobic interaction. Plenum Press, New York

Denning D, Patel S, Uversky V, Fink A, Rexach M (2003) Disorder in the nuclear pore complex: the FG repeat regions of nucleoporins are natively unfolded. Proc Natl Acad Sci USA 100(5): 2450–2455. doi:10.1073/pnas.0437902100

Dill KA (1985) Theory for the folding and stability of globular proteins. Biochemistry 24(1501):1501. doi:10.1021/bi00327a032

Fisher ME (1971) Critical phenomena. In: Green MS (ed) Proceedings of the Enrico Fermi Summer School. Academic Press, New York

Flory PJ (1941) Molecular size distribution in three dimensional polymers. J Am Chem Soc 63:3083

Flory PJ (1947) Principles of polymer chemistry. Cornell University Press, Ithaca

Frey S, Richter RP, Görlich D (2006) FG-rich repeats of nuclear pore proteins form a three-dimensional meshwork with hydrogel-like properties. Science 314:3

Görlich D, Kutay U (1999) Transport between the cell nucleus and the cytoplasm. Annu Rev Cell Dev Biol 15:607–660

Hurt EC (1988) A novel nucleoskeletal-like protein located at the nuclear periphery is required for the life cycle of *Saccharomyces cerevisiae*. EMBO J 7:4323

Iovine MK, Watkins JL, Wente SR (1995) The GLFG repetitive region of the nucleoporin Nup116p interacts with Kap95p, an essential yeast nuclear import factor. J Cell Biol 131:1699

Kyte J, Doolittle RF (1982) A simple method for displaying the hydropathic character of a protein. J Mol Biol 157:105132

Macara IG (2001) Transport into and out of the nucleus microbiol. Mol Biol Rev 65:570–594. doi:10.1128/MMBR.65.4.570-594.2001

Pemberton LF, Paschal BM (2005) Mechanisms of receptor-mediated nuclear import and nuclear export. Traffic 6:187

Peters R (2006) Introduction to nucleocytoplasmic transport: molecules and mechanisms. Methods Mol Biol 322:23558

Radu A, Blobel G, Moore MS (1995) Identification of a protein complex that is required for nuclear protein import and mediates docking of import substrate to distinct nucleoporins. Proc Natl Acad Sci USA 92(5):1769–1773

Ribbeck K, Görlich D (2001) Kinetic analysis of translocation through nuclear pore complexes. EMBO J 20:1320

Ribbeck K, Görlich D (2002) The permeability barrier of nuclear pore complexes appears to operate through hydrophobic exclusion. EMBO J 21:2664

Rout MP, Wente SR (1994) Pores for thought: nuclear pore complex proteins trends. Cell Biol 4:357

Rout MP, Aitchison JD, Suprapto A, Hjertaas K, Zhao A, Chait BT (2000) The yeast nuclear pore complex: composition, architecture and mechanism. J Cell Biol 148:635–652

Sahimi M (1994) Applications of percolation theory. Taylor & Francis, New York

Stauffer D, Amnon A (1992) Introduction to percolation systems. Taylor & Francis, New York

Stockmayer WH (1943) Theory of molecular size distribution and gel formation in branched polymers. J Chem Phys 11:45

Weis K (2002) Nucleocytoplasmic transport: cargo trafficking across the border. Curr Opin Cell Biol 14(3):328–335